



Expression of Programmed Cell Death-Ligands in Hepatocellular Carcinoma: Correlation With Immune Microenvironment and Survival Outcomes

Haotian Liao¹, Wen Chen², Yunlu Dai³, Joseph J. Richardson⁴, Junling Guo^{5*}, Kefei Yuan^{6*}, Yong Zeng^{1,6*} and Kunlin Xie¹

OPEN ACCESS

Edited by:

Giovanna Schiavoni,
Istituto Superiore di Sanità (ISS), Italy

Reviewed by:

Graham Robert Leggatt,
University of Queensland, Australia

Yan Wu,

Sun Yat-sen University, China

Dong-Ming Kuang,

Sun Yat-sen University, China

*Correspondence:

Junling Guo
junling.guo@wyss.harvard.edu

Kefei Yuan

ykf13@163.com

Yong Zeng

zengyong@medmail.com.cn

Specialty section:

This article was submitted to
Cancer Immunity and Immunotherapy,
a section of the journal
Frontiers in Oncology

Received: 05 April 2019

Accepted: 27 August 2019

Published: 11 September 2019

Citation:

Liao H, Chen W, Dai Y, Richardson JJ,
Guo J, Yuan K, Zeng Y and Xie K
(2019) Expression of Programmed
Cell Death-Ligands in Hepatocellular
Carcinoma: Correlation With Immune
Microenvironment and Survival
Outcomes. *Front. Oncol.* 9:883.
doi: 10.3389/fonc.2019.00883

¹ Liver Transplantation Division, Department of Liver Surgery, West China Hospital, Sichuan University, Chengdu, China, ² Department of Biological Chemistry and Molecular Pharmacology, Harvard Medical School, Boston, MA, United States, ³ Faculty of Health Sciences, University of Macau, Macau, China, ⁴ Department of Chemical and Biomolecular Engineering, ARC Centre of Excellence in Convergent Bio-Nano Science and Technology, University of Melbourne, Parkville, VIC, Australia, ⁵ John A. Paulson School of Engineering and Applied Sciences, Wyss Institute for Biologically Inspired Engineering, Harvard University, Boston, MA, United States, ⁶ Laboratory of Liver Surgery, West China Hospital, Sichuan University, Chengdu, China

The quantity of programmed cell death-ligand 1 (PD-L1) is regarded as a predicting factor of clinical response to anti-PD-1 axis immunotherapy. However, the expression of PD-L1 and its prognostic value in hepatocellular carcinoma (HCC) patients remain debated. Meanwhile, the molecular features of PD-1's other ligand, namely PD-L2, as well as its correlation with clinicopathological parameters and HCC tumor microenvironment (TME), are still poorly understood. In this study, immunohistochemistry (IHC) data from 304 HCC patients were used to determine the clinicopathological features of PD-L1 and PD-L2 and their correlation with CD8⁺ T cells in HCC. Moreover, fresh clinical HCC samples were used to identify the immune cell subtypes expressing PD-L1 and PD-L2. By using The Cancer Genome Atlas (TCGA) dataset, we further assessed the correlation between mutation signature, copy number variation (CNV), number of neoepitopes, immune gene expression, immune/stromal cell infiltration to the expression of PD-L1 and PD-L2. While membrane expression of PD-L2 was observed in 19.1% of tumor samples, no obvious expression of PD-L1 was detected on tumor cell membranes. High expression of PD-L2 on tumor membranes and PD-L1 in immune stroma were both significantly associated with poorer overall survival (OS) and disease-free survival (DFS) outcomes. Flow cytometry analysis and immunofluorescence showed that macrophages were the main immune cell subtype expressing both PD-L1 and PD-L2. Moreover, positive expression of PD-Ls was correlated with higher CD8⁺ T cells infiltration in immune stroma. CNV analysis showed a similarity between PD-L1 and PD-L2 in affecting gene expression. In addition, higher levels of PD-Ls correlated with higher

expression of immune related genes, enhanced cytolytic activity, and larger proportions of immune/stromal cell infiltration. Collectively, our study reveals the impact of both PD-L1 and PD-L2 on the HCC tumor microenvironment for the first time, providing insight for new therapeutic options.

Keywords: programmed cell death-ligands, macrophage, tumor immune stroma, tumor microenvironment, anti-PD-1 axis therapy, hepatocellular carcinoma

INTRODUCTION

Hepatocellular carcinoma (HCC) has recently become the second leading cause of cancer death around the world (1). Once diagnosed with HCC, only a small fraction of patients at early stages can benefit from curative treatments, including resection, local ablation or liver transplantation. While it has been reported that sorafenib can modestly extend the median survival of HCC patients at advanced stages (2), poor tolerance, and limited benefits due to relatively high drug resistance make the use of sorafenib a palliative care. Therefore, it's highly desirable to expand the therapeutic arsenal for HCC treatment.

Recently, the development of immune checkpoint inhibitors, which are capable of promoting the immune system to attack cancer cells, has experienced remarkable success (3). The interactions between the programmed death receptor 1 (PD-1) and programmed cell death-ligand 1 and 2 (PD-L1 and PD-L2) can induce T-cell exhaustion, which allows tumor cells to evade the immune system, leading to the failure of autoimmunity (4, 5). Thus, blocking PD-1 and PD-L1 association has become a key target for cancer immunotherapy. Two PD-1 inhibitors (Pembrolizumab and Nivolumab) and three PD-L1 (Atezolizumab, Avelumab, and Durvalumab) inhibitors have been approved, with others being tested in clinical trials at this moment.

Although the antitumor activity of PD-1 and PD-L1 inhibitors has been proved in various cancers (6–9), the clinical response to these therapies varies in different tumor types due to different PD-1 and PD-L1 behavior in individual patients. Therefore, significant efforts have been targeted toward finding predictive biomarkers to improve the identification of patients with potentially high therapeutic efficiency. The expression of PD-L1 in tumors, a main factor to determine the eligibility of patients for PD-1 axis targeted treatments, is conventionally detected by immunohistochemistry (IHC). However, a large proportion of PD-L1-positive patients have responded poorly to anti-PD-1 axis therapies, while some PD-L1-negative patients have unexpectedly

shown favorable therapeutic responses (10–14), suggesting that molecular interactions involving PD-1 independent from PD-L1 could also serve as predicting factors in the clinical responsiveness to these therapies. As another PD-1 ligand, PD-L2 is also commonly detected in human tumors, especially with its expression observed in the absence of PD-L1. Therefore, PD-L2 holds great value for predicting clinical response to anti-PD-1 axis therapies (11, 15–17). The expression of PD-L1 in HCC patients and its correlation with clinicopathological parameters have been fully illustrated. However, investigation of PD-1/PD-L2 interactions in HCC is still lacking (18, 19). The molecular features of both ligands, and their correlation with clinicopathological parameters and the tumor microenvironment (TME), are still poorly understood.

In this study, we aimed to define the biological and clinical relevance of the expressions of PD-L1 and PD-L2, as well as their correlation with each other in HCC. We used tissue microarrays (TMA) to examine 304 HCC tumor samples and analyzed the genomics data of HCC patients from The Cancer Genome Atlas (TCGA). The clinical and histopathological features of PD-L1 and PD-L2 in HCC tumor samples were assessed by IHC. Their precise locations in immune cell subtypes were detected by flow cytometry and immunofluorescence. Moreover, we evaluated how PD-L1 and PD-L2 expression are associated with transcriptomic profiles, copy number variation (CNV), and somatic mutations. These findings warrant further study focusing on both PD-L1 and PD-L2 as biomarkers of clinical outcomes to PD-1 blockade in HCC patients. Meanwhile, our work also provided a rationale for developing more effective anti-PD-1 axis immunotherapies for HCC.

MATERIALS AND METHODS

Patients and Samples

A total of 304 HCC patients undergoing hepatectomy between 2007 and 2012 in West China Hospital were included in this study. Tissue cores punched from representative tissue areas of formalin-fixed, paraffin-embedded (FFPE) HCC samples were selected to the construct tissue microarray (TMA). Tumor staging classification was carried out according to the 7th AJCC TNM Staging for Liver and Intrahepatic Bile Duct Malignancies. The characteristics of tumor samples including differentiation, size, number of nodules, vascular invasion, and Ishak fibrosis score of the adjacent liver tissue were evaluated by two pathologists specializing in hepatic diseases. The primary end point of this study was overall survival (OS), which was defined as the time from the date of surgery to the date of death

Abbreviations: PD-L1, programmed cell death-ligand 1; PD-L2, programmed cell death-ligand 2; PD-1, programmed death receptor 1; HCC, hepatocellular carcinoma; TME, tumor microenvironment; IHC, immunohistochemistry; TCGA, The Cancer Genome Atlas; OS, overall survival; DFS, disease-free survival; CNV, copy number variation; HBV, hepatitis B virus; HCV, hepatitis C virus; FFPE, formalin-fixed, paraffin-embedded; AFP, α -fetoprotein; IF, immunofluorescence; TPM, transcripts per million; CPM, count per million; SMGs, significantly mutated genes; BMR, background mutation rate; FDR, false discovery rate; WES, whole exome sequencing; GEO, Gene Expression Omnibus; HR, hazard ratio; LEL, lymphoepithelioma-like; CAFs, cancer associated fibroblasts; TECs, tumor endothelial cells; TAMs, tumor-associated macrophages; TILs, tumor infiltrating lymphocytes; IFN γ , interferon γ .

without regard to the cause of death. The secondary end point was disease-free survival (DFS) defined as the time from the date of surgery to the time of the first event (recurrence, progression, death). Patients with no events were censored at the date of their last follow-up. Informed consent for the use of tissue for the purpose of biomedical research was provided by every individual patient, with the approval from the ethics committee of West China Hospital.

Immunohistochemistry

TMA tissue sections were deparaffinized in xylene and rehydrated by sequential incubation in EtOH/water solutions. Antigen retrieval was conducted by heating the sections under high pressure in EDTA antigen retrieval solution against antibodies PD-L1 (1/400, Cell Signaling Technology), PD-L2 (1/400, R&D Systems), and CD8 (1/100, Abcam). The sections were incubated overnight at 4°C for primary antibodies. Then peroxidase reagents were used to limit steric interference and provide enhanced accessibility of secondary antibodies to the target. Envision system (enzyme-conjugated polymer backbone coupled to secondary antibodies) and 3, 3'-diaminobenzidine (DAB) chromogen were applied to perform the staining. Placenta tissues were used as a positive control for both PD-L1 and PD-L2 expressions. Negative controls included the use of PBS instead of primary antibodies, with all other conditions preserved. TMA images were viewed and captured using the NDP.view.2 software program. Slides were reviewed by two experienced pathologists who were blind to the clinical parameters. The expressions of PD-L1, PD-L2 were evaluated in tumor cells and tumor-infiltrating immune cells in HCC stroma. Expression of PD-L1 in immune stroma were recorded as the total number of cells expressing the protein in five respective areas at 40× magnification from each immunostained HCC section. Positive staining of PD-L1 in stroma was defined as the number of positive cells being higher than the median of the full series. The same strategy was used to record the expression of PD-L2 and CD8 in stroma. Positive staining of PD-L1 and PD-L2 in tumor cells was verified if staining of more than the membrane/surface was observed on over 1% of the tumor cells (20, 21).

Immunofluorescence

Immunofluorescence (IF) staining was performed on FFPE HCC tissue samples as previously described (22). The used antibodies are listed as follows, anti-PD-L1 (1,100, Cell Signaling Technology), anti-PD-L2 (1,100, R&D system), anti-CD8 (1,100, Abcam), and anti-CD68 (1,50, Santa Cruz). The corresponding secondary antibodies (Molecular Probes) were applied sequentially, and DAPI (Sigma) was used for nuclear staining. All images were acquired via Zeiss Axio Imager.

Flow Cytometry

Peripheral blood samples from untreated patients with pathologically confirmed HCC were obtained before curative resection. After surgical resection of the HCC, fresh tumor samples and adjacent normal tissues were taken and cut into small pieces, then enzymatically digested with 0.05% collagenase IV (Sigma-Aldrich), 0.002% DNase I (Roche), and 20% FBS

(HyClone Laboratories) in RPMI1640 medium (Gibco) at 37°C for 20 min. The resulting suspension was passed through 70 μm cell strainers (BD bioscience). The red blood cells in peripheral blood, HCC, and adjacent normal tissues were lysed using 1× Lysing Buffer (BD bioscience). The following fluorophore conjugated antibodies were used for flow cytometry, anti-CD3 (APC, BD bioscience), anti-CD4 (Alexa Fluor 700, BD bioscience), anti-CD8 (APC cy7, BD bioscience), anti-CD45RO (BV510, BD bioscience), anti-HLA-DR (PE-cy5, BD bioscience), anti-CD14 (FITC, BD Biosciences), anti-lin1 (FITC, Biolegend), anti-CD11c (APC, BD Biosciences), anti-CD123 (PE-cy7, BD Biosciences), anti-PD-L1 (BV421, BD Biosciences), and anti-PD-L2 (PE, BD Biosciences). Cells were incubated with antibodies in the dark for 30 min at 4°C in PBS + 1% BSA + 10% FBS. An aqua live/dead viability stain (Invitrogen) was added before flow cytometry analysis using the BD FACSDiva software. In order to relieve the effect of non-specific background signal when distinguishing PD-L1⁺ and PD-L2⁺ macrophages, various controls, including negative controls, isotype controls, and single staining controls (only one type of PD-Ls antibody was added, either PD-L1 or PD-L2), were used in our study.

Statistical Analysis

The significance of associations between PD-L1 and PD-L2 expression, as well as the associations between PD-Ls and CD8 expression, were assessed by the χ^2 test. Survival rates of expression level (low vs. high) were estimated by the Kaplan-Meier method with Rothman CIs. Survival curves were compared with the log-rank test. The hazard ratio (HR) and 95% CI associated with the expressions of PD-L1, PD-L2, and CD8 were estimated through a multivariable Cox regression model adjusted for TNM stage (I vs. II-III), HBV infection (no vs. yes), tumor size (≤ 5 vs. > 5 cm) and microvascular invasion (no vs. yes). Statistical analyses and graphics were conducted using R version 3.3.2.

RESULTS

PD-Ls Expression and Correlation With Clinicopathological Features of HCC Patients

The characteristics of patients are listed in **Table 1**. The median age of the patients was 49 years (ranging from 18 to 79 years old). Patients were dominated by male (82.9%) and a large proportion of patients were HBV-positive (84.9%). The presence of PD-L1 and PD-L2 in either tumor cell membranes or immune stroma was observed in 80 (26.3%) and 101 (33.2%) of the tumor samples, respectively. To our surprise, while membrane expression of PD-L2 was observed in 58 (19.1%) of tumor samples (**Figure 1A**, **Table 1**), no obvious expression of PD-L1 was detected on tumor cell membranes. Moreover, positive status of PD-L2 on tumor cell membranes was significantly associated with poorer OS and DFS (**Figure 1B**, both $P < 0.0001$). Regarding the expression in stromal immune cells, both PD-L1 and PD-L2 were detected in 80 (26.3%) and 59 (19.4%) of the tumor samples, respectively (**Figure 1C**, **Table 1**). While the expressions

TABLE 1 | Baseline characteristics of HCC patients.

Characteristic	Total N = 304
Male	252
Age, Median (range), y	49 (18–79)
HBV infection	
No	46
Yes	258
TNM stage	
I	141
II–III	163
Tumor differentiation	
Well	172
Poor	132
Tumor size, cm	
≤5	160
>5	144
Tumor multiplicity	
Single	246
Multiple	58
Microvascular invasion	
No	229
Yes	75
Portal vein thrombosis	
No	260
Yes	44
Liver cirrhosis	
No	115
Yes	189
α-Fetoprotein, ng/mL	
≤20	113
>20	191
PD-L1 in stroma	
Negative	224
Positive	80
PD-L2 in stroma	
Negative	245
Positive	59
PD-L2 in tumor cell	
Negative	246
Positive	58
CD8 TIL⁺ in stroma	
Negative	176
Positive	128
PD-L1⁺/PD-L2⁻ in stroma	47
PD-L1⁻/PD-L2⁺ in stroma	26
PD-L1⁻/PD-L2⁻ in stroma	198
PD-L1⁺/PD-L2⁺ in stroma	33

of PD-L1 in immune stroma were associated with poorer OS/DFS outcomes (**Figure 1D**, upper panel, $P < 0.0001$ and $P = 0.0019$, respectively), no statistically significant correlation was found between PD-L2 expression in immune stroma and OS/DFS outcomes (**Figure 1D**, lower panel, $P = 0.08$ and $P =$

0.056, respectively). Moreover, there are HCC samples exhibiting discordance between PD-L1 and PD-L2 in immune stroma, in which some displayed PD-L1 expression in the absence of PD-L2, while the rest showed the opposite (**Figure 1E**, **Table 1**). Nevertheless, a positive correlation was observed between PD-L1 and PD-L2 expressed by stromal immune cells (**Figure 1F**, left panel, $P < 0.0001$).

The association of combined PD-Ls expression in immune stroma with survival outcomes was also investigated (**Figure S1**). Significant differences in OS and DFS were found between patients with neither PD-L1 nor PD-L2 expressions and the other two groups of patients (PD-L1⁺PD-L2⁻/PD-L1⁻PD-L2⁺ and PD-L1⁺PD-L2⁺, respectively). Further statistical analysis demonstrated that there was a significant difference in the prevalence of PD-L2 on tumor cell membranes between PD-L1-positive and -negative samples (**Figure 1F**, right panel, $P = 0.013$). In addition, a strong correlation was observed between the mRNA expression levels of PD-L1 and PD-L2 in TCGA and GEO datasets (**Figure S2**). These findings suggested the high frequency of the co-existence of PD-L1 and PD-L2 in HCC. On the other hand, multivariate analysis showed that both PD-L1 in immune stroma and PD-L2 on tumor cell membranes were independent risk factors for OS and DFS (**Table 2**).

PD-Ls Expression in Immune Cell Subsets of Human HCC

Previous study has shown that macrophages were the predominant PD-L1⁺ population of immune cells in the HCC microenvironment (23), however the subtype of immune cells expressing PD-L2 in HCC remains unknown. It has been reported that PD-L2 can be expressed by various immune cell subtypes in response to microenvironmental stimulation, including two major antigen-presenting cells (APC), dendritic cells (DCs), macrophages, and T cells (24–28). Therefore, we analyzed the prevalence of PD-L2 expression in these immune cell subtypes and its correlation with PD-L1. The results showed the enrichment of CD4⁺ and CD8⁺ T cells in HCC tissue (**Figure S3A**). While lin⁻HLA-DR⁺ CD4⁺ CD11c⁺ CD123⁻ myeloid dendritic cells (mDCs) could be detected, lin⁻HLA-DR⁺ CD4⁺ CD11c⁻ CD123⁺ plasmacytoid dendritic cells (pDCs) were absent in HCC tissue (**Figure S3B**). Regarding the immune cell subtypes expressing PD-Ls, no obvious expression of PD-L1 or PD-L2 was observed in CD4⁺ T cells, CD8⁺ T cells, or mDCs (**Figures S3A,B**). However, both PD-L1 and PD-L2 could be found in HLA-DR⁺CD14⁺ macrophages (**Figure 2A**). Together with the previous study (23), our findings indicated that macrophages were the predominant population expressing PD-Ls in HCC microenvironment. In some cases, Neither PD-L1 nor PD-L2 were presented in macrophages (**Figure 2A**). Moreover, the percentages of PD-L1⁺ PD-L2⁻, PD-L1⁻ PD-L2⁺, and PD-L1⁺ PD-L2⁺ macrophages were all higher in tumor tissues than adjacent normal tissue and peripheral blood (**Figures 2A–C**). Meanwhile, the results demonstrated that macrophages were more numerous in HCC tissues than in the corresponding peripheral blood and adjacent normal tissues, suggesting the aggregation of PD-Ls⁺ macrophages in tumor tissue

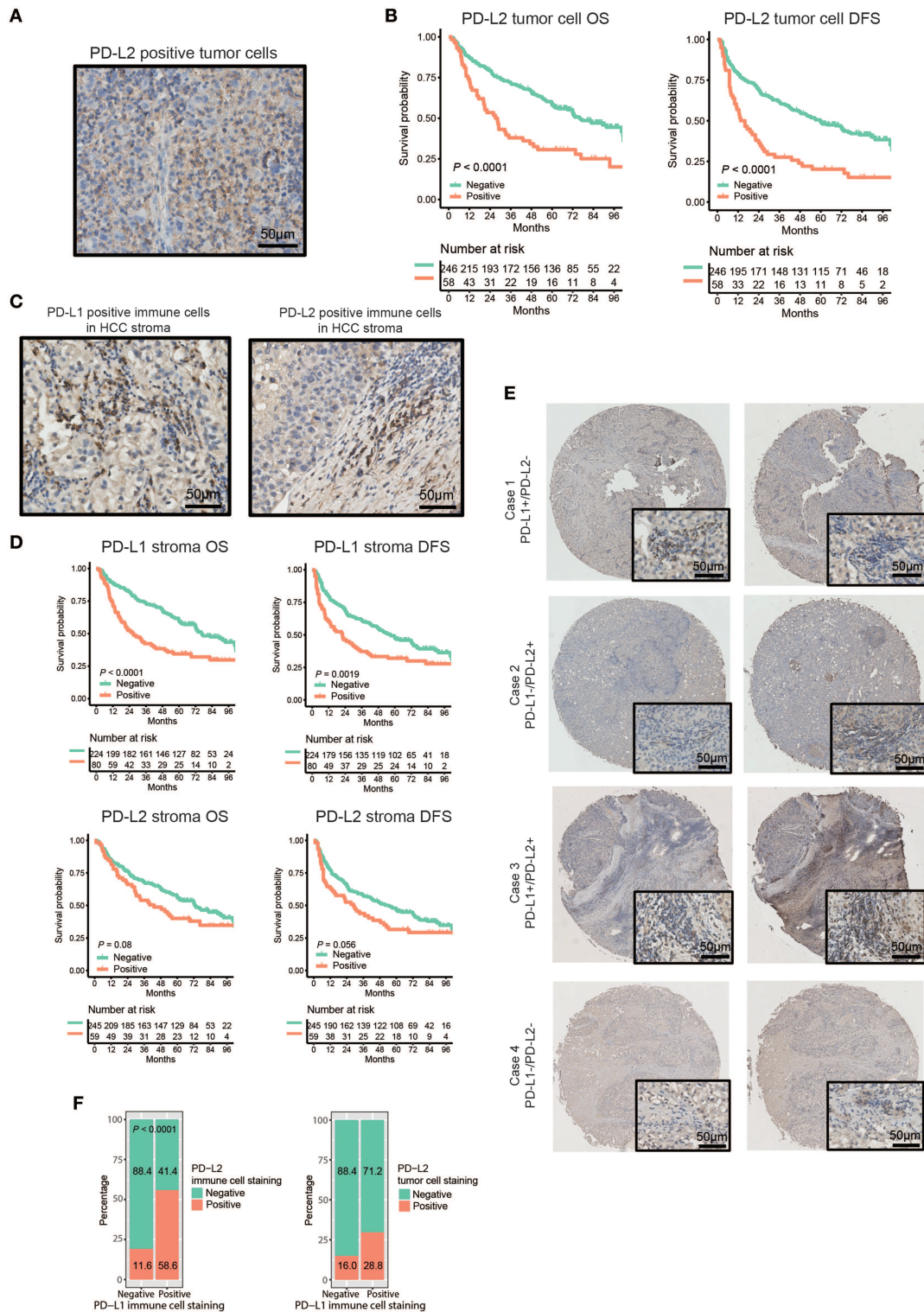


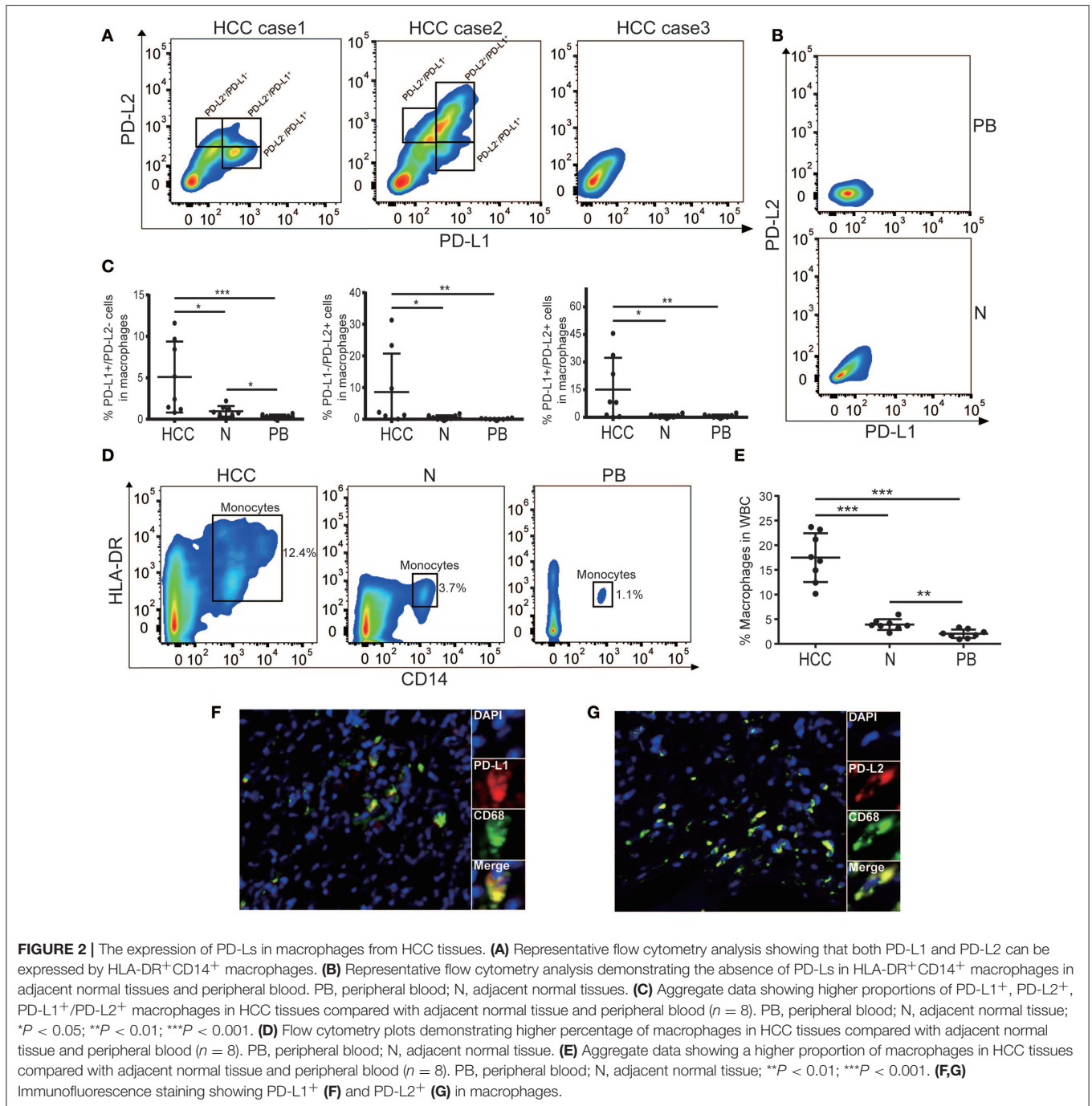
FIGURE 1 | Distribution and expression of PD-Ls and their correlation with prognosis in HCC patients. **(A)** IHC staining of PD-L2 on tumor cell membrane. **(B)** Kaplan-Meier curve of OS and DFS stratified by PD-L2 expression on tumor cell membrane. **(C)** IHC staining of PD-L1 and PD-L2 in immune stromal cells. **(D)** Kaplan-Meier curve of OS and DFS stratified by PD-L1, PD-L2 expression in immune stroma. **(E)** Representative images showing the association between expression of PD-L1 and PD-L2 in immune stroma. **(F)** Proportions of HCC tumor samples expressing PD-L2 in immune stroma (left panel) and on tumor cell membranes (right panel) stratified by PD-L1 expression in immune stroma.

TABLE 2 | Cox proportional hazard model showing hazard ratios for survival outcomes conferred by variables.

Variables	Overall survival				Disease-free survival			
	Univariate		Multivariate		Univariate		Multivariate	
	HR(95% CI)	P-value	HR(95% CI)	P-value	HR(95% CI)	P-value	HR(95% CI)	P-value
Sex								
Male	1(Ref)	0.479			1(Ref)	0.505		
Female	0.862(0.571–1.301)				0.877(0.596–1.290)			
Age								
≤60	1(Ref)	0.336			1(Ref)	0.246		
>60	1.165(0.854–1.589)				1.189(0.887–1.594)			
HBV infection								
No	1(Ref)	0.311			1(Ref)	0.723		
Yes	0.8149(0.549–1.210)				0.932(0.633–1.373)			
TNM stage								
I	1(Ref)	<0.0001	1(Ref)	0.012	1(Ref)	0.0001	1(Ref)	0.051
II-III	2.073(1.508–2.848)		1.642(1.114–2.419)		1.773(1.320–2.380)		1.442(0.999–2.082)	
Tumor differentiation								
Well	1(Ref)	0.106			1(Ref)	0.184		
Poor	1.285(0.945–1.741)				1.215(0.911–1.619)			
Tumor size, cm								
≤ 5	1(Ref)	<0.0001	1(Ref)	0.020	1(Ref)	0.0016	1(Ref)	0.088
> 5	1.907(1.403–2.594)		1.509(1.067–2.134)		1.587(1.190–2.116)		1.299(0.961–1.757)	
Tumor multiplicity								
Single	1(Ref)	0.003	1(Ref)	0.388	1(Ref)	0.013	1(Ref)	0.588
Multiple	1.719(1.204–2.455)		1.188(0.804–1.755)		1.537 (1.093–2.161)		1.108(0.763–1.608)	
Microvascular invasion								
No	1(Ref)	0.001	1(Ref)	0.404	1(Ref)	0.0008	1(Ref)	0.163
Yes	1.767(1.260–2.478)		1.184(0.796–1.762)		1.721(1.250–2.370)		1.307(0.897–1.904)	
Portal vein thrombosis								
No	1(Ref)	0.009	1(Ref)	0.248	1(Ref)	0.078		
Yes	1.712(1.145–2.558)		1.301(0.833–2.031)		1.421(0.961–2.101)			
Liver cirrhosis								
No	1(Ref)	0.586			1(Ref)	0.419		
Yes	1.029(0.749–1.413)				1.132(0.838–1.529)			
α-Fetoprotein, ng/mL								
≤20	1(Ref)	0.119			1(Ref)	0.157		
>20	1.292(0.936–1.785)				1.243(0.919–1.682)			
PD-L1 in stroma								
Negative	1(Ref)	<0.0001	1(Ref)	<0.0001	1(Ref)	0.002	1(Ref)	
Positive	1.992(1.436–2.763)		2.326(1.644–3.289)		1.632(1.192–2.233)		1.785(1.284–2.480)	0.0005
PD-L2 in stroma								
Negative	1(Ref)	0.081			1(Ref)	0.057		
Positive	1.384 (0.960–1.996)				1.399(0.989–1.979)			
PD-L2 in tumor cell								
Negative	1(Ref)	<0.0001	1(Ref)	0.0001	1(Ref)	<0.0001	1(Ref)	<0.0001
Positive	2.077(1.465–2.944)		2.027(1.407–2.921)		2.234(1.605–3.110)		2.244(1.587–3.172)	
CD8⁺ TIL in stroma								
Negative	1(Ref)	0.012	1(Ref)	0.0002	1(Ref)	0.011	1(Ref)	0.0008
Positive	0.666(0.485–0.914)		0.532(0.380–0.743)		0.682(0.506–0.918)		0.5880.430–0.803)	

(Figures 2D,E). Further validation by immunofluorescence also showed that both PD-L1 and PD-L2 could be expressed by macrophages in stroma (Figures 2F,G). These results indicated

that there was an accumulation of tumoral macrophages expressing both PD-L1 and PD-L2, potentially contributing to carcinogenesis in the HCC microenvironment.



CD8⁺ T Cell Infiltration in HCC and Its Association With the Expression of PD-Ls

Anti-PD-1 therapy accomplishes antitumor activity by blocking PD-1 in effector immune cells (such as CD8⁺ T cells) from interacting with their ligands, PD-L1/PD-L2 (29, 30). Most patients who benefited from anti-PD-1 therapy tended to have CD8⁺ T cell infiltration and higher PD-L1 expression in tumor tissue, and the expression of PD-L1 was significantly associated with CD8 density (31). Moreover, it has been reported that

PD-L1 was predominantly expressed in the lymphoepithelioma-like subtype of HCC (LEL-HCC), which is characterized by sheets of neoplastic cells intermingled with a dense immune stroma made of cytotoxic T (CD8⁺) cells (20, 32, 33). These findings suggested a potential interaction between PD-Ls and CD8⁺ T cell infiltration in HCC immune stroma. Thus, we evaluated the association between CD8 and PD-Ls (both PD-L1 and PD-L2) in HCC immune stroma. Consistent with the previous studies (20, 32, 33), a similar pattern of CD8⁺ T cell infiltration in immune

stroma was found in 128 (42.1%) tumor samples (**Figure 3A**, **Table 1**). Moreover, we found that patients with positive PD-L1 and/or PD-L2 expression tended to be of CD8 positive status, suggesting the co-existence of PD-L1⁺, PD-L2⁺ macrophages, and CD8⁺ T cells. Representative images from four cases were shown to illustrate the correlation between PD-L1, PD-L2 status, and CD8 expression in immune stroma (**Figure 3B**). Indeed, analysis on the protein expression in immune stroma (**Figure 3C**, PD-L1 vs. CD8, $P = 0.0012$; PD-L2 vs. CD8, $P < 0.0001$) and the mRNA level from TCGA and GEO datasets (**Figure S4**) showed that both PD-L1 and PD-L2 were positively associated with CD8 expression. Survival curve analysis showed that there was a positive correlation of CD8 expression with superior OS/DFS outcomes (**Figure S5**, **Table 2**). Moreover, the OS and DFS outcomes of PD-L1⁻/CD8⁺ patients were significantly better than other groups (**Figures 3D,E**), and PD-L1⁺/CD8⁻ status predicted poorer survival outcomes when compared with other groups (**Figures 3D,E**). These results were similar to what was found when stratifying patients into different subgroups based on PD-L2/CD8 expression, in which PD-L2⁻/CD8⁺ patients had a relatively better prognosis than other groups, while the prognosis of PD-L2⁺/CD8⁻ patients was poorer (**Figures 3E,G**).

Mutational Event and CNV Analysis in Patients With High vs. Low Expression of PD-Ls

An accurate landscape of the mutations in HCC driver genes has been provided by previous genetic profiling studies (34). Therefore, we sought to evaluate whether PD-Ls correlated with distinct mutational profiles characterized for HCC (**Supplementary Materials**). While no statistical difference could be identified in mutations between tumors with high and low PD-L1 expression, PD-L2-high tumors had a slightly higher mutation burden in TP53 (**Figures 4A,B**, χ^2 test, $P < 0.05$). In the meantime, most mutations across the dataset were associated with G>A and C>T transitions, and higher frequencies of A>G and T>C transitions were observed in tumors low in PD-L1 (**Figure S6A**). However, the frequency of specific substitutions did not differ between PD-L2-high and -low tumors (**Figure S6B**).

Previous studies have demonstrated increased genomic instability with extensive CNV in HCC patients (34–37), so we then assessed CNV between HCC subtypes with different expression of PD-Ls through GISTIC 2.0 analysis (**Supplementary Materials**). We discovered that a large number of cytobands were either significantly amplified or deleted regardless of the influence by PD-L1 or PD-L2 expression (**Figures 5A,B**). Both PD-L1-high and PD-L2-high subjects had 1024 genes within the chromosome regions with significant copy number amplification. After overlaying these genes with the differentially expressed genes identified by RNAseq, PD-L1-high and PD-L2-high subgroups had 57 and 52 genes within the amplification regions showing a concordant expression pattern in RNAseq, respectively (**Figure 5C**, upper panel). This implied that the different expression patterns of these genes were partially owing to copy number amplification. On the other hand, the

numbers of genes within the deletion regions in PD-L1-high and PD-L2-high subgroups were both 676. Meanwhile, both PD-L1-high and PD-L2-high subgroups had 29 genes within the deletion regions showing a concordant expression pattern in RNAseq, suggesting that different expression patterns of these genes could partially due to the copy number deletion (**Figure 5D**, upper panel). In addition, for genes with different expression patterns owing to copy number amplification, there was an overlap between PD-L1-high group and PD-L2-high group (43 genes, **Figure 5C**, lower panel). Such behavior was similar to genes that attributed their different expression pattern to copy number deletion (26 genes, **Figure 5D**, lower panel). These findings suggested the potential similarity between the up-regulations of PD-L1 and PD-L2 in affecting CNV, which finally leads to the differential expression of these genes.

Correlation Among Neopeptide Loads, Cytolytic Activity, Cytokine Gene Expressions, and the Expression of PD-Ls

Neopeptides are peptides that arise from somatic mutations and are entirely absent from the normal human genome. They are reported to preferentially drive the T cell recognition of tumor cells (38). Therefore, we determined whether PD-Ls correlated with neopeptide loads in HCC (**Supplementary Materials**). This analysis revealed no correlation between total mutations per individual tumor and expression of PD-Ls (**Figure 6A**). Meanwhile, when viewed as a group, tumors with higher expression of PD-Ls exhibited no increase in the number of total mutations when compared to those with lower expression of PD-Ls (**Figure 6A**). In regard to neopeptide loads, no association was found between neopeptide loads and the expression of PD-Ls (**Figure 6B**). These findings suggested that the expression of PD-Ls is not driven by increased mutations or neopeptide loads.

Previous studies have provided evidence for immunoediting in tumors and have uncovered the mechanisms of tumor-intrinsic resistance to cytolytic activity by using large-scale genomic data sets of solid tissue tumor biopsies (36, 39). In this study, we also analyzed the potential of PD-Ls expression in affecting cytolytic activity. Cytolytic activity was defined as the geometric mean of GZMA and PRF1 (expressed in TPM, **Supplementary Materials**). We found that there is a strong correlation between cytolytic activity and the expression of PD-Ls (both PD-L1 and PD-L2) in HCC patients (**Figure 6C**), suggesting that immune response in cytolytic-high HCC samples can elicit tumor mechanisms of immune suppression regulated by PD-Ls.

Increasing evidence suggests that pro-inflammatory and anti-inflammatory cytokine imbalances are widely in existence in the tumor microenvironment. The presence of such imbalances promote the development and progression of HCC (40, 41). Moreover, it has been determined that engagement of PD-1 by PD-Ls dramatically affects T cell receptor (TCR)-mediated and cytokine production (24, 42). We hypothesized that expression of these cytokines, chemokines, and interleukins are dysregulated in HCC tumors with higher expression

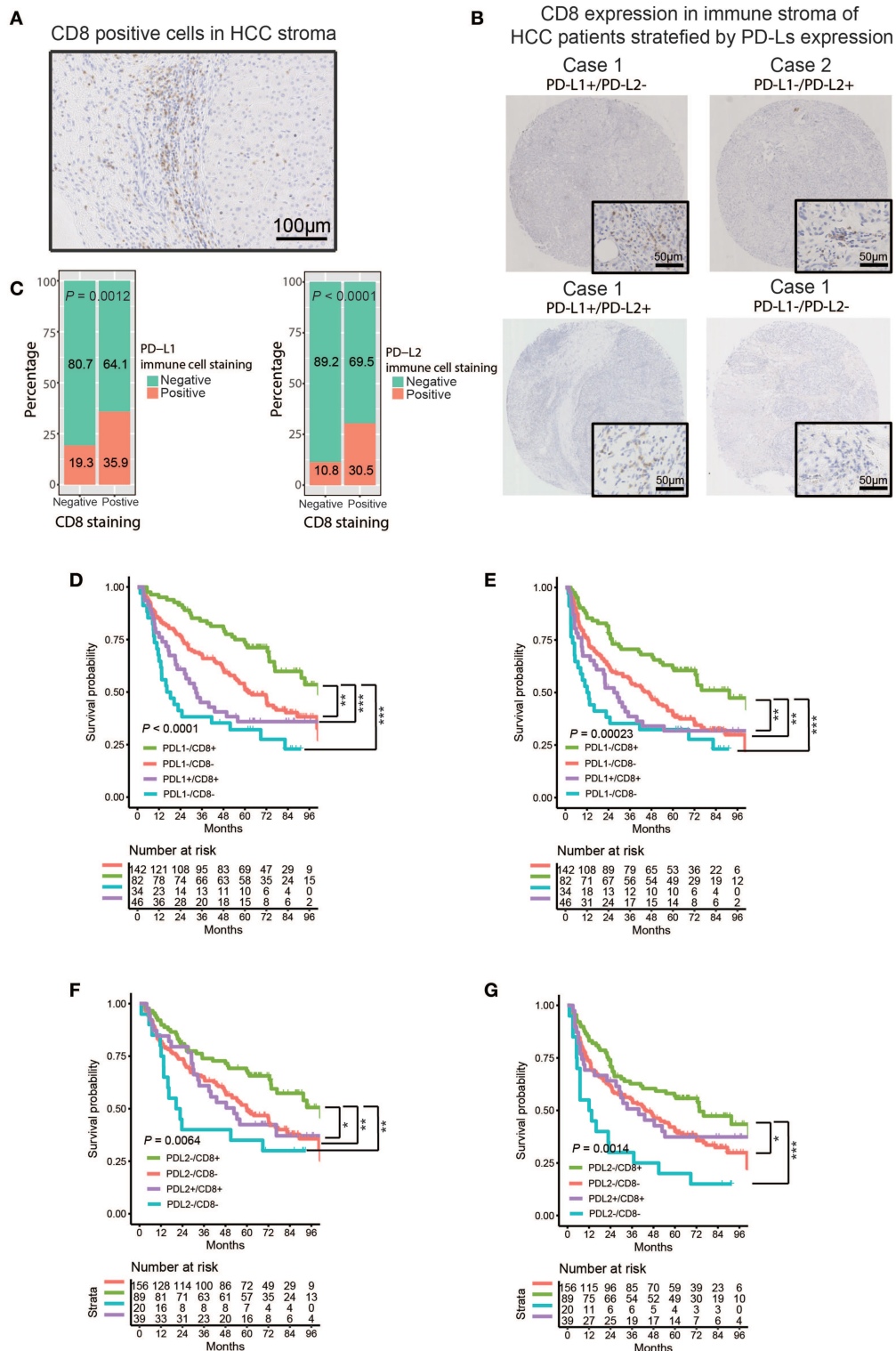


FIGURE 3 | Correlation between PD-Ls and CD8⁺ T cell infiltration in HCC immune stroma. **(A)** Representative images showing CD8 expression in HCC immune stroma. **(B)** Representative CD8 expression in immune stroma of HCC patients stratified by PD-Ls expression. **(C)** Proportions of HCC tumor samples expressing CD8 stratified by PD-L1 and PD-L2 expressed by immune stroma. **(D–G)** Kaplan-Meier curves of OS **(D, E)** and DFS **(F, G)** stratified by PD-L1 (left panel) and PD-L2 (right panel) in combination with CD8 expression in immune stroma. * $P < 0.05$; ** $P < 0.01$; *** $P < 0.001$.

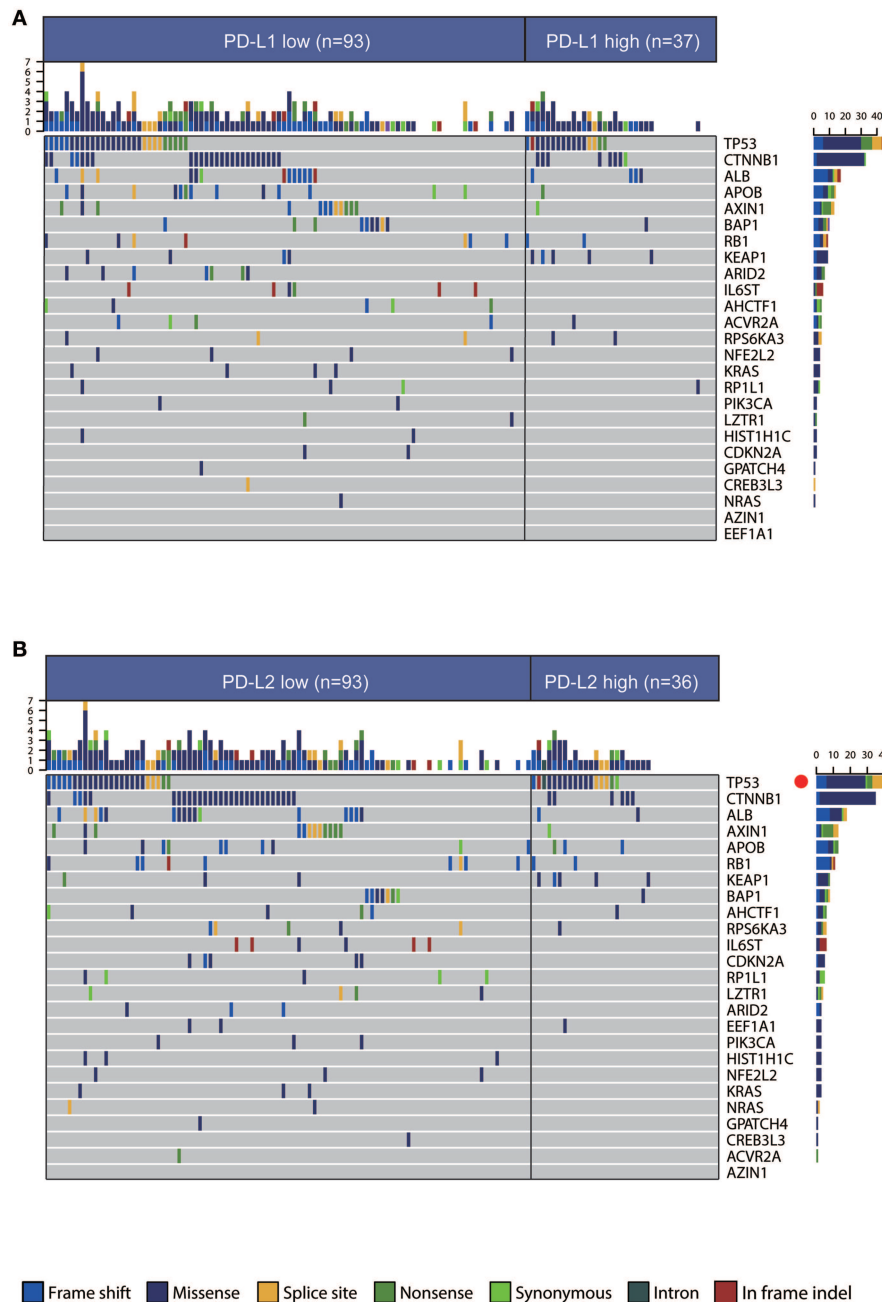


FIGURE 4 | Association between PD-Ls and mutational signatures in HCC. **(A,B)** Significantly mutated genes in HCC subsets stratified by PD-L1 **(A)** and PD-L2 **(B)** expression. Red dot, $P < 0.05$.

of PD-Ls (**Supplementary Materials**). Consistently, we found that the expression of various pro- and anti-inflammatory cytokines was significantly increased in PD-Ls-high tumors (**Figure 6D**). Cytokines were previously shown to be the positive regulators of HCC progression, including CXCL5, IFNG, CCL5, PLAUG, PTN, CSF1, and HGF, and they were significantly up-regulated in tumors with higher PD-L1 or PD-L2 expression (43–49). There are also other cytokines inhibiting

the progression of HCC, including IL15, IL18, and CD40LG. Our findings indicated there are conflicts between pro- and anti-inflammatory cytokines in promoting HCC progression. Meanwhile, the expression of regulatory T cell (Treg) markers was also up-regulated in tumors with higher expression of PD-Ls (**Figures S7A,B**). Evaluation of other immune checkpoints pathways showed that multiple inhibitory checkpoint molecules (except for ADORA2A) including PD-1 were at statistically

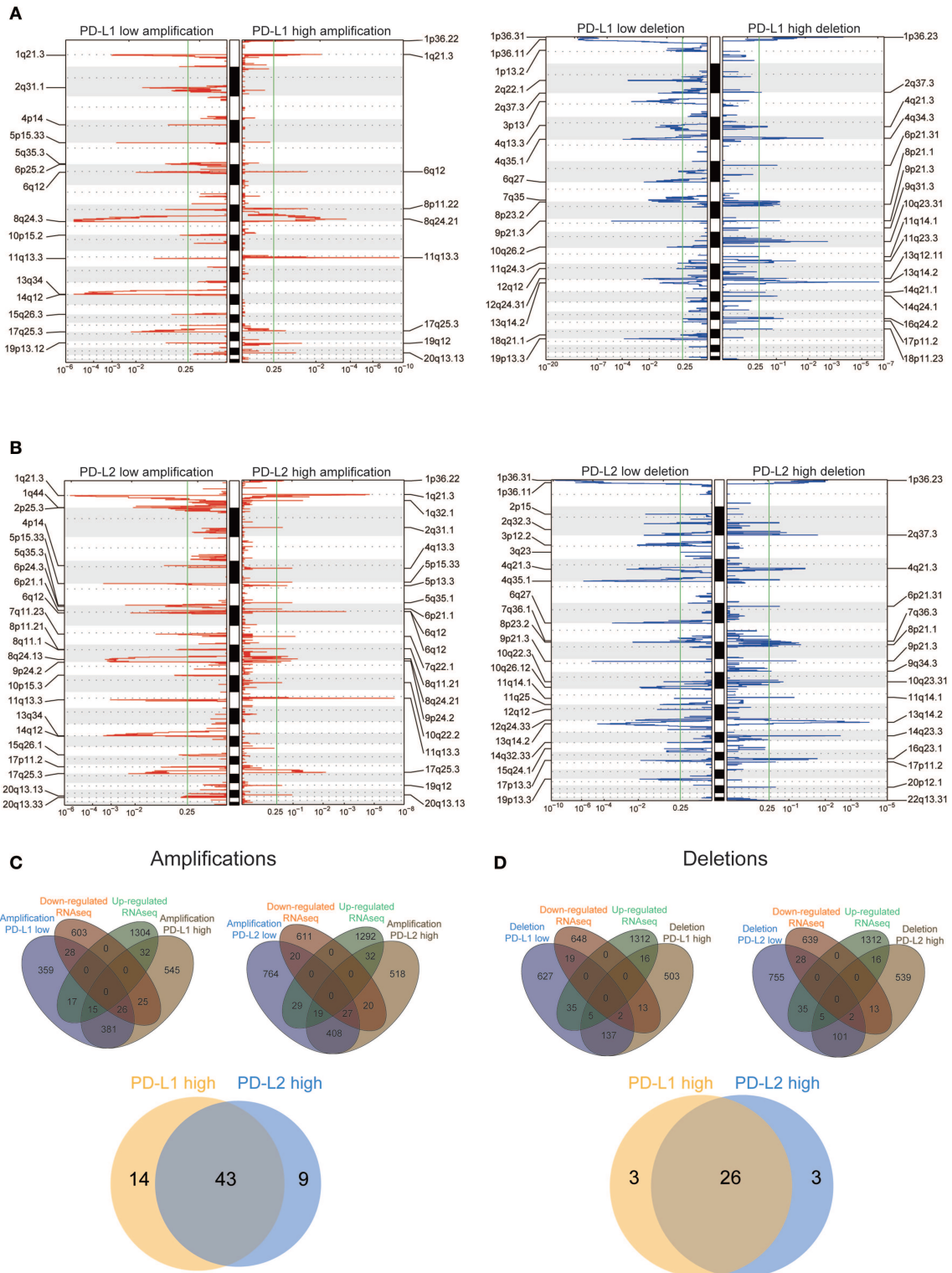


FIGURE 5 | Association between PD-Ls and CNV in HCC. **(A,B)** GISTIC2.0 analysis identified recurrent somatic copy number alterations in different HCC subsets stratified by PD-L1 **(A)** and PD-L2 **(B)** expression. **(C,D)** Venn diagrams demonstrating the number of genes within genomic regions showing significant amplification or deletion, as well as the overlay with significant genes identified from RNAseq in different HCC subsets stratified by PD-L1 **(C)** and PD-L2 **(D)** expression. Each circle in the Venn diagram represents one set and the number in the overlaid area represents the common genes between the sets.

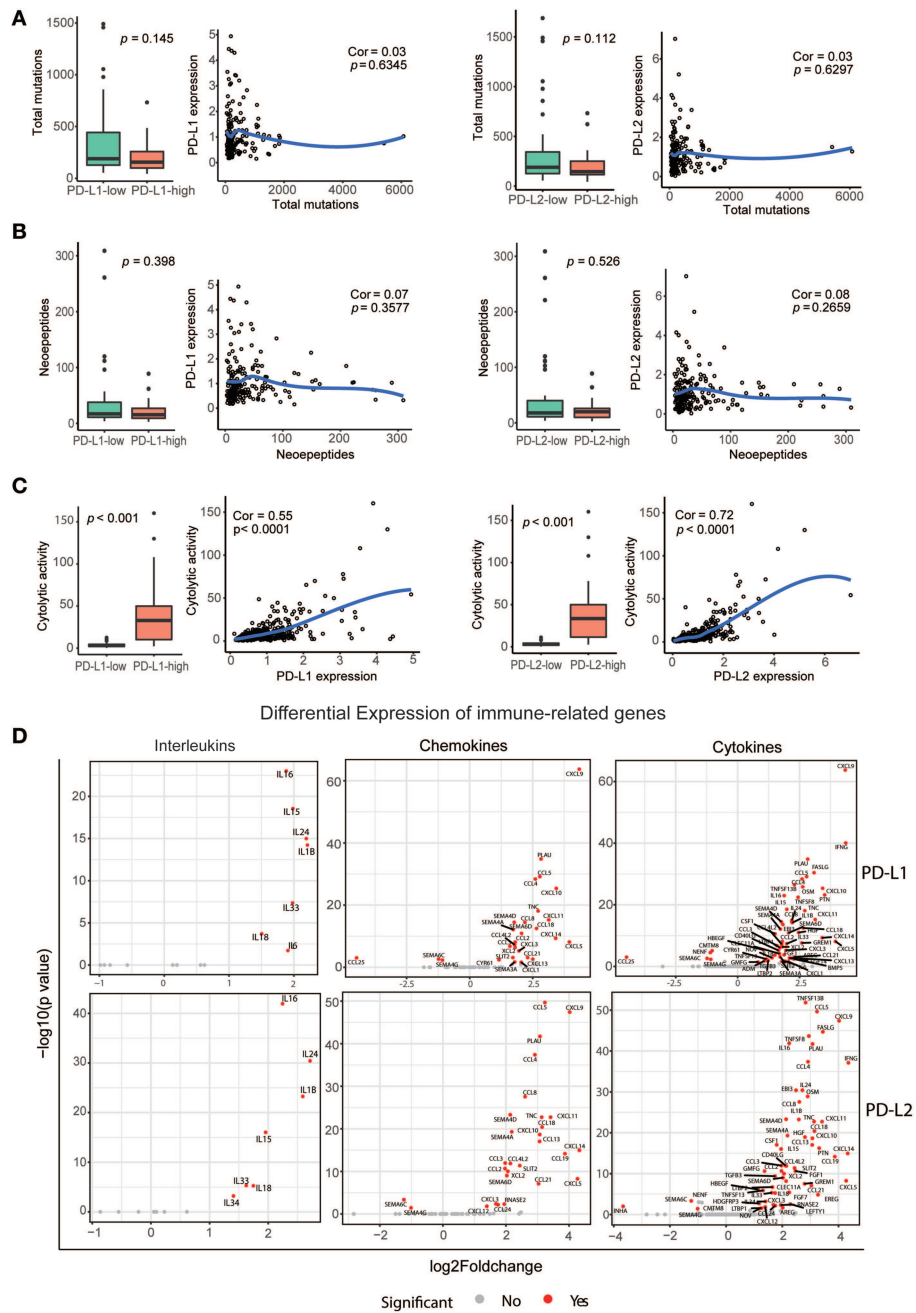


FIGURE 6 | Correlation between PD-Ls and neopeptide loads, cytolytic activity, and immune gene expression. **(A)** Local regression curves (Spearman rank correlation) between expression of PD-Ls and total mutation count; boxplot distributions between HCC subsets stratified by the expression of PD-Ls (Mann-Whitney). **(B)** Local regression curves between the expression of PD-Ls and numbers of neopeptides and boxplot distributions between HCC subsets stratified by the expression of PD-Ls. **(C)** Local regression curves between the expression of PD-Ls and cytolytic activity and boxplot distributions between HCC subsets stratified by PD-Ls expression. **(D)** Differentially expressed cytokines between PD-Ls-high and -low HCC samples.

higher levels in tumors with higher PD-L1 or PD-L2 expression (Figures S8A,B). These data suggested that the cooperation between PD-1 axis and other immune checkpoint pathways are common in mediating peripheral tolerance and immune escape in HCC.

Tissue-Infiltrating Immune/Stromal Cell Populations in HCC Tumors With High vs. Low PD-Ls Expression

It has been hypothesized that within the tumor microenvironment, the recognition of cancer-associated

antigens by CD8⁺ T cells can lead to the local production of IFN- γ , which ultimately induces the adaptive expression of PD-L1 on neighboring tumor infiltrating immune cells and tumor cells (5, 50–52). To analyze the correlation between immune cell infiltration and PD-Ls expression in HCC, the abundance of tissue-infiltrating immune and non-immune stromal cell populations in patients with different expression of PD-Ls (PD-L1 low vs. high; PD-L2 low vs. high) were evaluated by using the R package MCPcounter [Supplementary Materials; (53)]. A distinct distribution of immune and stromal cell types was found between different HCC subtypes, in which tumors with higher PD-L1 or PD-L2 expression had more abundant infiltrating immune cells, including natural killer (NK)-cells, monocytes, B cells, different types of T cells, dendritic cells, and certain types of stromal cells (fibroblasts and endothelial cells) (Figure 7). In order to determine the association of PD-Ls with immune cell function, we analyzed the enrichment data of six immune function gene sets as reported previously (36). The results showed that PD-L1 (Figure S9A) demonstrated a strong correlation with co-inhibition by antigen presenting cells (APC, Cor = 0.494), while PD-L2 (Figure S9B) demonstrated strong correlations with: (i) co-inhibition by APCs (Cor = 0.620); (ii) co-inhibition by T cells (Cor = 0.545), and (iii) co-stimulation by T cells (Cor = 0.512).

DISCUSSION

The roles of PD-Ls in predicting survival outcomes of HCC patients remains controversial. Gao et al. reported that higher expressions of PD-L1 and PD-L2 in tumor cells were associated with poorer survival outcomes of HCC patients. However, the study of Sideras et al. showed that PD-L1 expressed by tumor cells correlates with superior survival outcomes (54). In this study, we found that the higher expression of PD-L1 in HCC stroma was associated with poorer survival outcomes. It is worth noticing that previous studies have mainly focused on the association between the expression of PD-Ls in HCC tumor cells and survival outcomes. While positive PD-L1 staining could also be observed in HCC tumor cells, it's hard to distinguish positive stainings on membranes from those in cytoplasm, which was consistent with the report from previous study (18). Thus, no positive PD-L1 staining was recorded due to the methods used in our work (Materials and Methods). Therefore, only PD-L1-positive status in HCC tumor stroma has been recorded. On the other hand, the expression of PD-L2 could be detected in both HCC tumor cells and immune stroma. In addition to the fact that the frequency of PD-L2 expression is higher than PD-L1 in tumor cells (55), our findings are more clinically relevant because anti-PD-L1 treatment alone has a lower response rate than anti-PD-1 (12 and 27%, respectively) (16, 56). While no statistically significant correlation was found between PD-L2 expression in immune stroma and OS/DFS outcomes (Figure 1D, lower panel), two subgroups of patients with different survival outcomes based on PD-L2 in stroma can be easily identified from the survival curves. Considering statistically significant correlation of PD-L1 with OS/DFS (Figure 1D, upper panel), this result might be

partially owing to the discordance between PD-L1 and PD-L2 expressions in over 40% of the patients included. In order to confirm that the antibodies used in this study could provide correct staining pattern in IHC tissues, placental tissue was used as a positive control. The results demonstrated the selective PD-L1 and PD-L2 staining of the syncytiotrophoblast layer in placental tissue, validating the excellent status of antibodies in all of our experiments (Figure S10). Therefore, our results play a pivotal role in ending the controversy surrounding the different distributions of PD-L1 and PD-L2 in the HCC tumor microenvironment.

It is well-established that the development and progression of cancer is regulated by genetic and epigenetic alterations in the transformed cells. However, many steps in carcinogenesis, including proliferation, invasion and angiogenesis, have been proven to be manipulated by tumor stroma, which consists of cancer associated fibroblasts (CAFs), tumor endothelial cells (TECs) and tumor-associated macrophages (TAMs) (57). On the other hand, while most cancer research has focused on the mutations in oncogenes or tumor suppressor genes that promote cancer formation, it has been widely perceived that the non-malignant cells in the tumor microenvironment progress along with the tumor cells and can provide support for their malignant phenotype (58). Among the normal cells in the tumor microenvironment, macrophages have been demonstrated to be the most abundant (59). Rather than exhibiting antitumor effects after being activated *in vitro*, macrophages acquire a protumoral phenotype *in vivo* (60, 61). These facts have highlighted the immune function of macrophages in cancer immune stroma and the importance of understanding their roles and potential mechanisms in tumor immunopathogenesis. For the first time, our study observed the co-existence of PD-L1 and PD-L2 in macrophages within HCC immune stroma. Our results also showed that both PD-L1 and PD-L2 in immune stroma are independent prognostic factors for OS along with the well-established factors including TNM stage and tumor size. These findings strongly suggest the pro-oncogenic role of macrophages in HCC immune stroma.

Currently, the association between the expression of PD-Ls and tumor infiltrating lymphocytes (TILs) has been reported in various cancers (52, 62, 63). Expression of PD-L1 on tumor cells or macrophages can reduce Granzyme B and IFN- γ expressed by CD8⁺ T cells, leading to the dysfunction of cytolytic activity in CD8⁺ T cells (64). Considering the overlapping functions of PD-L1 with PD-L2, this fact highly suggests that both PD-L1 and PD-L2 regulate cytolytic functions of CD8⁺ T cells. Although the infiltration of CD8⁺ TILs in HCC tissue has been reported, no study has ever focused on the correlation between CD8⁺ TILs and the expression of PD-Ls in HCC immune stroma ever since the co-existence of CD8 and PD-L1 in LEL-HCC was validated (20). Therefore, research on the correlation between CD8⁺ TILs and PD-Ls is of great significance. Consistent with previous studies (32), small clusters of CD8⁺ TILs were observed in HCC immune stroma. At the same time, the expression of PD-Ls positively correlated with CD8⁺ TIL infiltration. Further supported by the facts that both PD-L1 and PD-L2 were predominantly expressed

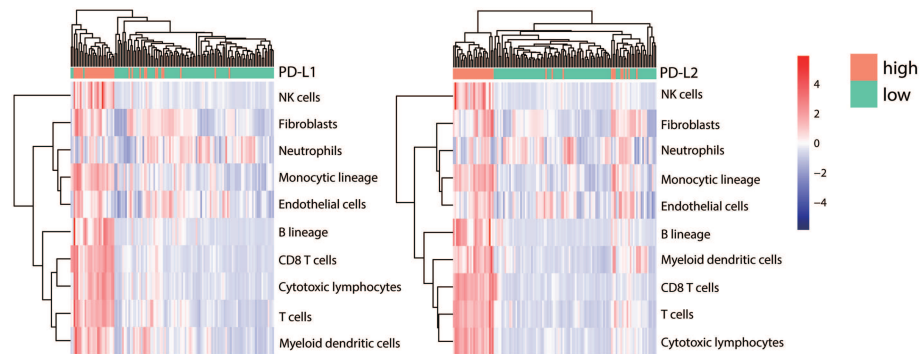


FIGURE 7 | Correlation between PD-Ls and immune/stromal cell infiltration. The proportions of infiltrating immune and stromal cells between HCC subsets stratified by PD-L1 (left panel) and PD-L2 (right panel) expression. Unsupervised clustering shows the consistency between TILs infiltrating patterns and candidate grouping based on PD-Ls expression.

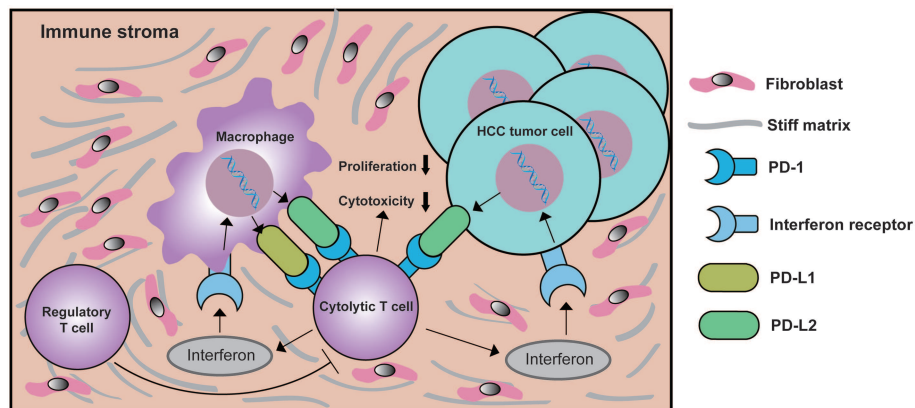


FIGURE 8 | Schematic depiction of the mechanisms underlying PD-Ls-mediated cytolytic T cell exhaustion in the HCC microenvironment. In response to interferon γ signaling activated by cytolytic T cell, macrophages in immune stroma up-regulate PD-L1 and/or PD-L2 expression. At the same time, the expression of PD-L2 on HCC tumor cell membranes is also increased. The ligation of PD-Ls in macrophage and HCC tumor cells with PD-1 will down-modulate the function of cytolytic T cells, thus eventually creating a negative feedback loop that inhibits the proliferation and cytotoxicity of cytolytic T cells, thus reducing antitumor immunity. During this process, the function of regulatory T cell (Treg) is enhanced, which further suppresses the function of cytolytic T cells.

by immune stromal cells from our study, we believe there is a strong correlation between the expression of PD-Ls and the infiltration of $CD8^+$ TILs in HCC immune stroma. After stratifying patients into different subgroups according to the expression of PD-Ls and CD8, we were able to identify patients with PD-Ls-negative status and $CD8^+$ TIL infiltration, suggesting other suppressor(s) could be involved in promoting immune tolerance (type IV tumors) according to the classification method raised by Teng et al. (65). The aforementioned patients have the best survival outcomes. Patients have the worst prognosis when showing expression of PD-Ls but no TIL infiltration, indicating the presence of tumors with oncogenic pathways induced by PD-Ls (type III tumors). Considering that macrophages are the predominant immune cell subtype expressing both PD-L1 and PD-L2, we propose a new mechanism of how macrophages regulate PD-Ls, during the progression of HCC, macrophages in immune stroma up-regulate PD-Ls in response to $IFN\gamma$ released by TILs as an adaptive immune-resistance

mechanism to suppress $CD8^+$ effector T cell function, thus leading to $CD8^+$ T cell exhaustion/inhibition and poorer survival outcomes (Figure 8).

PD-Ls' expression effect and the effect being impacted by anti-tumor immunity in the HCC microenvironment have not been systematically illustrated. Previous study on multiple tumor models demonstrated that, despite the accumulation of $CD8^+$ T cells and NK cells during tumor progression, the activation of these immune cells will be substantially inhibited by the binding of PD-Ls to them, which attenuates the anti-tumor activity of these cells (64). For the first time, we used large-scale transcriptional and genetic data to explore the genomic landscape of HCC in the context of different expression levels of PD-Ls. By stratifying patients based on expression of PD-Ls, we found higher levels of PD-Ls are correlated with higher expression of cytokines, immune checkpoint molecules, Treg markers, and higher cytolytic activity. These results indicate that tumors highly expression

PD-Ls are likely to possess pre-existing antitumor immunity. Therefore, they can subsequently arouse immune tolerance and initiate a feedback loop during the progression of HCC. On the other hand, the similarities between PD-L1 and PD-L2 in affecting CNV suggest their synergistic effect in regulating gene expression, potentially shaping the microenvironment within HCC tissue. Moreover, by using the R package MCPcounter, we found that, in HCC tissue, higher expression of PD-Ls was associated with a higher proportion of infiltration of immune cells, as well as stromal cells including fibroblasts and endothelial cells. Further validation by using Tumor Immune Estimation Resource (TIMER; cistrome.shinyapps.io/timer) (66) showed that a positive correlation between the expression of PD-Ls and tumor immune cell infiltration. However, a negative correlation between expression of PD-Ls and tumor purity is observed, suggesting that both PD-L1 and PD-L2 are expressed by non-cancerous cells mainly consisting of immune cells in the HCC tumor microenvironment (Figure S11). Combining these findings with the results obtained by immunohistochemistry, we can draw a conclusion that HCC tissue with a higher expression of PD-L1 or PD-L2 are affected and characterized by the existence of a substantial immune stroma consisting of various infiltrating immune cells. Taken together, our findings promote further understanding of the molecular pathology of PD-Ls in the HCC microenvironment.

CONCLUSION

In conclusion, this study has highlighted the essential role of PD-Ls expressed by macrophages in HCC immune stroma and their potency in regulating the tumor microenvironment. In addition, this study has provided potentially practical management options for future clinical trials on anti PD-1 axis therapy for HCC patients, it should be based on the expression of PD-L1, PD-L2, and CD8 along with the clinicopathological characteristics of HCC patients. Further studies will focus on the blockade of both PD-L1 and PD-L2 in macrophages for the immunotherapy of HCC.

REFERENCES

- Chen W, Zheng R, Baade PD, Zhang S, Zeng H, Bray F, et al. Cancer statistics in China, 2015. *CA Cancer J Clin.* (2016) 66:115–32. doi: 10.3322/caac.21338
- Llovet JM, Ricci S, Mazzaferro V, Hilgard P, Gane E, Blanc JF, et al. Sorafenib in advanced hepatocellular carcinoma. *N Engl J Med.* (2008) 359:378–90. doi: 10.1056/NEJMoa0708857
- Sharma P, Allison JP. The future of immune checkpoint therapy. *Science.* (2015) 348:56–61. doi: 10.1126/science.aaa8172
- Dai S, Jia R, Zhang X, Fang Q, Huang L. The PD-1/PD-Ls pathway and autoimmune diseases. *Cell Immunol.* (2014) 290:72–9. doi: 10.1016/j.cellimm.2014.05.006
- Pardoll DM. The blockade of immune checkpoints in cancer immunotherapy. *Nat Rev Cancer.* (2012) 12:252–64. doi: 10.1038/nrc3239
- Hodi FS, O'Day SJ, McDermott DF, Weber RW, Sosman JA, Haanen JB, et al. Improved survival with ipilimumab in patients with metastatic melanoma. *N Engl J Med.* (2010) 363:711–23. doi: 10.1056/NEJMoa1003466

DATA AVAILABILITY

Publicly available datasets were analyzed in this study. This data can be found here: <https://portal.gdc.cancer.gov/>

ETHICS STATEMENT

This study was carried out in accordance with the recommendations of guideline in human sample research from the ethics committee of West China Hospital. Informed consent for the use of tissue for the purpose of biomedical research was provided by every individual patient, with the approval from the ethics committee of West China Hospital.

AUTHOR CONTRIBUTIONS

YZ, KY, and JG designed this study. HL and WC performed the experiments. HL performed statistical analysis and write the manuscript. YD, JR, and KX helped revising the manuscript. All authors read and approved the final manuscript.

FUNDING

This work was supported by grants from the Natural Science Foundation of China (81872004, 81800564, 81770615, 81700555, 81672882, and 81502441) and the Science and Technology Support Program of Sichuan Province (2017SZ0003, 2018SZ0115).

ACKNOWLEDGMENTS

We thank the TCGA working group for generating publicly available data.

SUPPLEMENTARY MATERIAL

The Supplementary Material for this article can be found online at: <https://www.frontiersin.org/articles/10.3389/fonc.2019.00883/full#supplementary-material>

- Motzer RJ, Escudier B, McDermott DF, George S, Hammers HJ, Srinivas S, et al. Nivolumab versus everolimus in advanced renal-cell carcinoma. *N Engl J Med.* (2015) 373:1803–13. doi: 10.1056/NEJMoa1510665
- Ribas A, Puzanov I, Dummer R, Schadendorf D, Hamid O, Robert C, et al. Pembrolizumab versus investigator-choice chemotherapy for ipilimumab-refractory melanoma (KEYNOTE-002): a randomised, controlled, phase 2 trial. *Lancet Oncol.* (2015) 16:908–18. doi: 10.1016/S1470-2045(15)00083-2
- Rizvi NA, Mazieres J, Planchard D, Stinchcombe TE, Dy GK, Antonia SJ, et al. Activity and safety of nivolumab, an anti-PD-1 immune checkpoint inhibitor, for patients with advanced, refractory squamous non-small-cell lung cancer (CheckMate 063): a phase 2, single-arm trial. *Lancet Oncol.* (2015) 16:257–65. doi: 10.1016/S1470-2045(15)70054-9
- Garon EB, Rizvi NA, Hui R, Leigh N, Balmanoukian AS, Eder JP, et al. Pembrolizumab for the treatment of non-small-cell lung cancer. *N Engl J Med.* (2015) 372:2018–28. doi: 10.1056/NEJMoa1501824
- Herbst RS, Soria JC, Kowanetz M, Fine GD, Hamid O, Gordon MS, et al. Predictive correlates of response to the anti-PD-L1 antibody MPDL3280A in cancer patients. *Nature.* (2014) 515:563–7. doi: 10.1038/nature14011

12. Robert C, Long GV, Brady B, Dutriaux C, Maio M, Mortier L, et al. Nivolumab in previously untreated melanoma without BRAF mutation. *N Engl J Med.* (2015) 372:320–30. doi: 10.1056/NEJMoa1412082
13. Robert C, Schachter J, Long GV, Arance A, Grob JJ, Mortier L, et al. Pembrolizumab versus ipilimumab in advanced melanoma. *N Engl J Med.* (2015) 372:2521–32. doi: 10.1056/NEJMoa1503093
14. Tumeu PC, Harview CL, Yearley JH, Shintaku IP, Taylor EJ, Robert L, et al. PD-1 blockade induces responses by inhibiting adaptive immune resistance. *Nature.* (2014) 515:568–71. doi: 10.1038/nature13954
15. Stevenson ML, Wang CQ, Abikhair M, Roudiani N, Felsen D, Krueger JG, et al. Expression of programmed cell death ligand in cutaneous squamous cell carcinoma and treatment of locally advanced disease with pembrolizumab. *JAMA Dermatol.* (2017) 153:299–303. doi: 10.1001/jamadermatol.2016.5118
16. Taube JM, Klein A, Brahmer JR, Xu H, Pan X, Kim JH, et al. Association of PD-1, PD-L1 ligands, and other features of the tumor immune microenvironment with response to anti-PD-1 therapy. *Clin Cancer Res.* (2014) 20:5064–74. doi: 10.1158/1078-0432.CCR-13-3271
17. Yearley JH, Gibson C, Yu N, Moon C, Murphy E, Juco J, et al. PD-L2 expression in human tumors: relevance to anti-PD-1 therapy in cancer. *Clin Cancer Res.* (2017) 23:3158–67. doi: 10.1158/1078-0432.CCR-16-1761
18. Gao Q, Wang XY, Qiu SJ, Yamato I, Sho M, Nakajima Y, et al. Overexpression of PD-L1 significantly associates with tumor aggressiveness and postoperative recurrence in human hepatocellular carcinoma. *Clin Cancer Res.* (2009) 15:971–9. doi: 10.1158/1078-0432.CCR-08-1608
19. Jung HI, Jeong D, Ji S, Ahn TS, Bae SH, Chin S, et al. Overexpression of PD-L1 and PD-L2 is associated with poor prognosis in patients with hepatocellular carcinoma. *Cancer Res Treat.* (2017) 49:246–54. doi: 10.4143/crt.2016.066
20. Calderaro J, Rousseau B, Amaddeo G, Mercey M, Charpy C, Costentin C, et al. Programmed death ligand 1 expression in hepatocellular carcinoma: relationship With clinical and pathological features. *Hepatology.* (2016) 64:2038–46. doi: 10.1002/hep.28710
21. Xie K, Xu L, Wu H, Liao H, Luo L, Liao M, et al. OX40 expression in hepatocellular carcinoma is associated with a distinct immune microenvironment, specific mutation signature, and poor prognosis. *Oncoimmunology.* (2018) 7:e1404214. doi: 10.1080/2162402X.2017.1404214
22. Mallone R, Funaro A, Zubiatur M, Baj G, Ausiello CM, Tacchetti C, et al. Signaling through CD38 induces NK cell activation. *Int Immunol.* (2001) 13:397–409. doi: 10.1093/intimm/13.4.397
23. Wu K, Kryczek I, Chen L, Zou W, Welling TH. Kupffer cell suppression of CD8+ T cells in human hepatocellular carcinoma is mediated by B7-H1/programmed death-1 interactions. *Cancer Res.* (2009) 69:8067–75. doi: 10.1158/0008-5472.CAN-09-0901
24. Latchman Y, Wood CR, Chernova T, Chaudhary D, Borde M, Chernova I, et al. PD-L2 is a second ligand for PD-1 and inhibits T cell activation. *Nat Immunol.* (2001) 2:261–8. doi: 10.1038/85330
25. Lesterhuis WJ, Punt CJ, Hato SV, Eleveld-Trancikova D, Jansen BJ, Nierkens S, et al. Platinum-based drugs disrupt STAT6-mediated suppression of immune responses against cancer in humans and mice. *J Clin Invest.* (2011) 121:3100–8. doi: 10.1172/JCI43656
26. Lesterhuis WJ, Steer H, Lake RA. PD-L2 is predominantly expressed by Th2 cells. *Mol Immunol.* (2011) 49:1–3. doi: 10.1016/j.molimm.2011.09.014
27. Messal N, Serriari NE, Pastor S, Nunes JA, Olive D. PD-L2 is expressed on activated human T cells and regulates their function. *Mol Immunol.* (2011) 48:2214–9. doi: 10.1016/j.molimm.2011.06.436
28. Wang S, Bajorath J, Flies DB, Dong H, Honjo T, Chen L. Molecular modeling and functional mapping of B7-H1 and B7-DC uncouple costimulatory function from PD-1 interaction. *J Exp Med.* (2003) 197:1083–91. doi: 10.1084/jem.20021752
29. Topalian SL, Hodi FS, Brahmer JR, Gettinger SN, Smith DC, McDermott DF, et al. Safety, activity, and immune correlates of anti-PD-1 antibody in cancer. *N Engl J Med.* (2012) 366:2443–54. doi: 10.1056/NEJMoa1200690
30. Woo SR, Corrales L, Gajewski TF. Innate immune recognition of cancer. *Annu Rev Immunol.* (2015) 33:445–74. doi: 10.1146/annurev-immunol-032414-112043
31. Eroglu Z, Zaretsky JM, Hu-Lieskovan S, Kim DW, Algazi A, Johnson DB, et al. High response rate to PD-1 blockade in desmoplastic melanomas. *Nature.* (2018) 553:347–50. doi: 10.1038/nature25187
32. Chan AW, Tong JH, Pan Y, Chan SL, Wong GL, Wong VW, et al. Lymphoepithelioma-like hepatocellular carcinoma: an uncommon variant of hepatocellular carcinoma with favorable outcome. *Am J Surg Pathol.* (2015) 39:304–12. doi: 10.1097/PAS.0000000000000376
33. Solinas A, Calvisi DF. Lessons from rare tumors: hepatic lymphoepithelioma-like carcinomas. *World J Gastroenterol.* (2015) 21:3472–9. doi: 10.3748/wjg.v21.i12.3472
34. Huber-Ruano I, Raventos C, Cuartas I, Sanchez-Jaro C, Arias A, Parra JL, et al. An antisense oligonucleotide targeting TGF-beta2 inhibits lung metastasis and induces CD86 expression in tumor-associated macrophages. *Ann Oncol.* (2017) 28:2278–85. doi: 10.1093/annonc/mdx314
35. Guichard C, Amaddeo G, Imbeaud S, Ladeiro Y, Pelletier L, Maad IB, et al. Integrated analysis of somatic mutations and focal copy-number changes identifies key genes and pathways in hepatocellular carcinoma. *Nat Genet.* (2012) 44:694–8. doi: 10.1038/ng.2256
36. Rooney MS, Shukla SA, Wu CJ, Getz G, Hacohen N. Molecular and genetic properties of tumors associated with local immune cytolytic activity. *Cell.* (2015) 160:48–61. doi: 10.1016/j.cell.2014.12.033
37. Sung WK, Zheng H, Li S, Chen R, Liu X, Li Y, et al. Genome-wide survey of recurrent HBV integration in hepatocellular carcinoma. *Nat Genet.* (2012) 44:765–9. doi: 10.1038/ng.2295
38. Schumacher TN, Schreiber RD. Neoantigens in cancer immunotherapy. *Science.* (2015) 348:69–74. doi: 10.1126/science.aaa4971
39. Balli D, Rech AJ, Stanger BZ, Vonderheide RH. Immune cytolytic activity stratifies molecular subsets of human pancreatic cancer. *Clin Cancer Res.* (2017) 23:3129–38. doi: 10.1158/1078-0432.CCR-16-2128
40. Budhu A, Wang XW. The role of cytokines in hepatocellular carcinoma. *J Leukoc Biol.* (2006) 80:1197–213. doi: 10.1189/jlb.0506297
41. Marra F, Tacke F. Roles for chemokines in liver disease. *Gastroenterology.* (2014) 147:577–94.e1. doi: 10.1053/j.gastro.2014.06.043
42. Hirahara K, Ghoreschi K, Yang XP, Takahashi H, Laurence A, Vahedi G, et al. Interleukin-27 priming of T cells controls IL-17 production in trans via induction of the ligand PD-L1. *Immunity.* (2012) 36:1017–30. doi: 10.1016/j.immuni.2012.03.024
43. Bai PS, Xia N, Sun H, Kong Y. Pleiotrophin, a target of miR-384, promotes proliferation, metastasis and lipogenesis in HBV-related hepatocellular carcinoma. *J Cell Mol Med.* (2017) 21:3023–43. doi: 10.1111/jcmm.13213
44. Buurman R, Gurlevik E, Schaffer V, Eilers M, Sandbothe M, Kreipe H, et al. Histone deacetylases activate hepatocyte growth factor signaling by repressing microRNA-449 in hepatocellular carcinoma cells. *Gastroenterology.* (2012) 143:811–20.e15. doi: 10.1053/j.gastro.2012.05.033
45. Cai H, Zhu XD, Ao JY, Ye BG, Zhang YY, Chai ZT, et al. Colony-stimulating factor-1-induced AIF1 expression in tumor-associated macrophages enhances the progression of hepatocellular carcinoma. *Oncoimmunology.* (2017) 6:e1333213. doi: 10.1080/2162402X.2017.1333213
46. Chan CF, Yau TO, Jin DY, Wong CM, Fan ST, Ng IO. Evaluation of nuclear factor-kappaB, urokinase-type plasminogen activator, and HBx and their clinicopathological significance in hepatocellular carcinoma. *Clin Cancer Res.* (2004) 10 (12 Pt 1):4140–9. doi: 10.1158/1078-0432.CCR-03-0574
47. Li H, Wu K, Tao K, Chen L, Zheng Q, Lu X, et al. Tim-3/galectin-9 signaling pathway mediates T-cell dysfunction and predicts poor prognosis in patients with hepatitis B virus-associated hepatocellular carcinoma. *Hepatology.* (2012) 56:1342–51. doi: 10.1002/hep.25777
48. Sasaki R, Devhare PB, Steele R, Ray R, Ray RB. Hepatitis C virus-induced CCL5 secretion from macrophages activates hepatic stellate cells. *Hepatology.* (2017) 66:746–57. doi: 10.1002/hep.29170
49. Zhou SL, Dai Z, Zhou ZJ, Wang XY, Yang GH, Wang Z, et al. Overexpression of CXCL5 mediates neutrophil infiltration and indicates poor prognosis for hepatocellular carcinoma. *Hepatology.* (2012) 56:2242–54. doi: 10.1002/hep.25907
50. Kim JM, Chen DS. Immune escape to PD-L1/PD-1 blockade: seven steps to success (or failure). *Ann Oncol.* (2016) 27:1492–504. doi: 10.1093/annonc/mdw217
51. Spranger S, Spaepen RM, Zha Y, Williams J, Meng Y, Ha TT, et al. Up-regulation of PD-L1, IDO, and T(regs) in the melanoma tumor microenvironment is driven by CD8(+) T cells. *Sci Transl Med.* (2013) 5:200ra116. doi: 10.1126/scitranslmed.3006504

52. Taube JM, Anders RA, Young GD, Xu H, Sharma R, McMiller TL, et al. Colocalization of inflammatory response with B7-h1 expression in human melanocytic lesions supports an adaptive resistance mechanism of immune escape. *Sci Transl Med.* (2012) 4:127ra37. doi: 10.1126/scitranslmed.3003689
53. Becht E, Giraldo NA, Lacroix L, Buttard B, Elarouci N, Petitprez F, et al. Estimating the population abundance of tissue-infiltrating immune and stromal cell populations using gene expression. *Genome Biol.* (2016) 17:218. doi: 10.1186/s13059-016-1070-5
54. Sideras K, Biermann K, Verheij J, Takkenberg BR, Mancham S, Hansen BE, et al. PD-L1, Galectin-9 and CD8(+) tumor-infiltrating lymphocytes are associated with survival in hepatocellular carcinoma. *Oncoimmunology.* (2017) 6:e1273309. doi: 10.1080/2162402X.2016.1273309
55. Giraldo NA, Becht E, Pages F, Skliris G, Verkarre V, Vano Y, et al. Orchestration and prognostic significance of immune checkpoints in the microenvironment of primary and metastatic renal cell cancer. *Clin Cancer Res.* (2015) 21:3031–40. doi: 10.1158/1078-0432.CCR-14-2926
56. Brahmer JR, Tykodi SS, Chow LQ, Hwu WJ, Topalian SL, Hwu P, et al. Safety and activity of anti-PD-L1 antibody in patients with advanced cancer. *N Engl J Med.* (2012) 366:2455–65. doi: 10.1056/NEJMoa1200694
57. Hofmeister V, Schrama D, Becker JC. Anti-cancer therapies targeting the tumor stroma. *Cancer Immunol Immunother.* (2008) 57:1–17. doi: 10.1007/s00262-007-0365-5
58. Joyce JA, Pollard JW. Microenvironmental regulation of metastasis. *Nat Rev Cancer.* (2009) 9:239–52. doi: 10.1038/nrc2618
59. Noy R, Pollard JW. Tumor-associated macrophages: from mechanisms to therapy. *Immunity.* (2014) 41:49–61. doi: 10.1016/j.immuni.2014.06.010
60. Biswas SK, Allavena P, Mantovani A. Tumor-associated macrophages: functional diversity, clinical significance, and open questions. *Semin Immunopathol.* (2013) 35:585–600. doi: 10.1007/s00281-013-0367-7
61. Fidler IJ. Macrophage therapy of cancer metastasis. *Ciba Found Symp.* (1988) 141:211–22. doi: 10.1002/9780470513736.ch12
62. Kim MY, Koh J, Kim S, Go H, Jeon YK, Chung DH. Clinicopathological analysis of PD-L1 and PD-L2 expression in pulmonary squamous cell carcinoma: comparison with tumor-infiltrating T cells and the status of oncogenic drivers. *Lung Cancer.* (2015) 88:24–33. doi: 10.1016/j.lungcan.2015.01.016
63. Velcheti V, Schalper KA, Carvajal DE, Anagnostou VK, Syrigos KN, Sznol M, et al. Programmed death ligand-1 expression in non-small cell lung cancer. *Lab Invest.* (2014) 94:107–16. doi: 10.1038/labinvest.2013.130
64. Lee YH, Martin-Orozco N, Zheng P, Li J, Zhang P, Tan H, et al. Inhibition of the B7-H3 immune checkpoint limits tumor growth by enhancing cytotoxic lymphocyte function. *Cell Res.* (2017) 27:1034–45. doi: 10.1038/cr.2017.90
65. Teng MW, Ngiow SF, Ribas A, Smyth MJ. Classifying cancers based on T-cell infiltration and PD-L1. *Cancer Res.* (2015) 75:2139–45. doi: 10.1158/0008-5472.CAN-15-0255
66. Li T, Fan J, Wang B, Traugh N, Chen Q, Liu JS, et al. TIMER: A web server for comprehensive analysis of tumor-infiltrating immune cells. *Cancer Res.* (2017) 77:e108–10. doi: 10.1158/0008-5472.CAN-17-0307

Conflict of Interest Statement: The authors declare that the research was conducted in the absence of any commercial or financial relationships that could be construed as a potential conflict of interest.

Copyright © 2019 Liao, Chen, Dai, Richardson, Guo, Yuan, Zeng and Xie. This is an open-access article distributed under the terms of the Creative Commons Attribution License (CC BY). The use, distribution or reproduction in other forums is permitted, provided the original author(s) and the copyright owner(s) are credited and that the original publication in this journal is cited, in accordance with accepted academic practice. No use, distribution or reproduction is permitted which does not comply with these terms.